Proceedings of the ASME 2010 International Design Engineering Technical Conferences & Computers and Information in Engineering Conference
IDETC/CIE 2010
August 15-18, 2010, Montreal, Quebec, Canada

DETC2010-29161

IN-SITU MONITORING AND PREDICTION OF PROGRESSIVE JOINT WEAR USING BAYESIAN STATISTICS

Dawn An
School of Aerospace & Mechanical Engineering, Korea Aerospace University
Goyang-City, Gyeonggi-do, Korea

Nam Ho Kim
Dept. of Mechanical & Aerospace Engineering, University of Florida
Gainesville, FL 32611, U.S.A.

Jooho Choi
School of Aerospace & Mechanical Engineering, Korea Aerospace University
Goyang-City, Gyeonggi-do, Korea

ABSTRACT

In this paper, a statistical methodology of estimating wear coefficient and predicting wear volume in a revolute joint using in-situ measurement data is presented. An instrumented slider-crank mechanism is built, which can measure the joint force and the relative motion between the pin and bushing during operation. The former is measured using a load cell built onto a necked portion of the hollow steel pin, while the latter is measured using a capacitance probe. In order to isolate the effect of friction in other joints, a porous carbon air bearing for the revolute joint between the follower link and the slide stage, as well as a prismatic joint for the linear slide, are used. Based on the relative motion between the centers of pin and bushing, the wear volumes are estimated at six different operating cycles. The Bayesian inference technique is used to update the distribution of wear coefficient, which incorporates in-situ measurement data to obtain the posterior distribution. In order to obtain the posterior distribution, Markov Chain Monte Carlo technique is employed, which effectively draws samples of the given distribution. The results show that it is possible to narrow the distribution of wear coefficient and to predict the future wear volume with reasonable confidences. The effect of prior distribution on the wear coefficient is discussed by comparing with non-informative case.

Keywords: wear, Bayesian inference, Markov Chain Monte Carlo, slider-crank mechanism.

1 INTRODUCTION

Mechanical systems are characterized by motion. In order to fulfill their design function, the individual components of a system must move relative to one another, which inevitably produces sliding along the mating surfaces and causes a destructive effect known as wear. Wear is the gradual removal of material from contacting surfaces in relative motion, which eventually causes failure of the system. Since wear inevitably exists for most of mechanical systems in motion, it is important to predict it and estimate the service life of the system before it fails due to wear.

The traditional practice of predicting service life of a mechanical component under wear is performed through two stages [1]. First, a wear coefficient of the material used is measured in a laboratory environment using the tribometer test. Normally, a constant load is applied on the two mating surfaces under rotational or reciprocating motion. Second, the contact pressure and sliding distance of an actual component are calculated using either analytical or numerical methods. Then, wear volume is estimated as a function of service life by combining the wear coefficient with contact pressure and sliding distance.

Although the above process is well-adopted, the fundamental limitation of wear prediction is that it works only with a constant contact pressure condition that is used in the tribometer test. In practice, however, the contact pressure usually varies as a function of time. Furthermore, it varies even within a contact surface. Since the wear coefficient is not an intrinsic material property, it varies with different operating conditions. Calculating wear coefficients at all possible operating conditions requires numerous wear tests and is extremely time consuming. In addition, the variability of wear coefficient is significant even if different parts are made of the same material. Recently, Mukras et al. [2] presented an integrated framework of predicting wear under variable kinematics and kinetics. It was found that the process is

computationally intensive to predict wear under varying loads and wear surfaces that change continuously.

Thus, it would be more desirable to measure the wear coefficient directly from the mechanical component used. Since calculating the wear coefficient requires kinematic information (wear volume and sliding distance) as well as kinetic information (contact force/pressure), it is important to design an in-situ measurement apparatus to measure both factors. In this paper, we used an instrumented slider-crank mechanism [3] to measure kinematic and kinetic information. Since in-situ measurement is often accompanied by various noises and errors, we used the Bayesian inference technique to update the statistical distribution of wear coefficient.

The paper is organized as follows. In Section 2, a simple wear model that is used in this paper is summarized. Although a linear model is used, the main concept of the paper can be extended to more complicated wear models. In Section 3, in-situ measurements of joint force and wear volume are presented. Section 4 presents the Bayesian inference technique along with the Markov Chain Monte Carlo (MCMC) method. In Section 5, the wear coefficient is statistically identified and validated, followed by conclusions and discussions in Section 6.

2 WEAR MODEL AND WEAR COEFFICIENT

Among different kinds of wear phenomena, it is assumed that all the wear cases to be predicted fall within the plastically dominated wear regime, where sliding velocities are small and surface heating can be considered negligible. The Archard's wear model [4] would thus serve as the appropriate wear model to describe the wear as discussed by Lim and Ashby [5] as well as Cantizano et al.[6]. The Archard's wear model assumes that the volume of material removed (ΔV) is linearly proportional to the product of the slip distance (d) and the normal load (F_n). The traditional method of calculating wear coefficient is shown schematically in Figure 1. In that model, first published by Holm [7], the worn-out volume, during the process of wear, is considered to be proportional to the normal load. The model is expressed mathematically as follows:

$$\frac{\Delta V}{s} = K\frac{F_n}{H} \tag{1}$$

where ΔV is the worn-out volume, s the slip distance, K the dimensionless wear coefficient, H the Brinell hardness of the softer material, and F_n the applied normal force. Since the wear coefficient is the quantity of interest, Eq. (1) is often written in the following form:

$$k = \frac{V}{F_n s} \tag{2}$$

The non-dimensioned wear coefficient K and the hardness are bundled up into a single dimensioned wear coefficient k. Since the worn-out volume is relatively small, it is often measured in the unit of mm^3. Thus, the unit of wear coefficient becomes [mm^3/N-m]. Note that the wear coefficient is not an intrinsic material property. The value of k for a specific operating condition and given pair of materials may be obtained through experimentation [1].

As can be expected from Figure 1, the applied normal force and contact area remain constant through the entire process. If the normal force varies within the slip distance, the definition of wear coefficient in Eq. (2) needs to be modified as

$$k = \frac{V}{\int_0^s F_n(s)\mathrm{d}s} \tag{3}$$

In the above definition, it is assumed that the wear coefficient is independent of normal force, which is generally not true. However, the wear coefficient k in Eq. (3) can be interpreted as an average wear coefficient for given load profile.

3 IN-SITU MEASUREMENT OF JOINT WEAR OF A SLIDER-CRANK MECHANISM

The crank-slider test apparatus used in the study is shown in Figure 2. The detailed dimensions of crank and slider are summarized in Table 1. The design philosophy is to attempt to isolate friction, wear and error motions exclusively to the joint under consideration. In order to minimize confounding dynamic contributions from the other components in the mechanism, a porous carbon air bearing for the revolute joint between the follower link and the slide stage, as well as a prismatic joint for

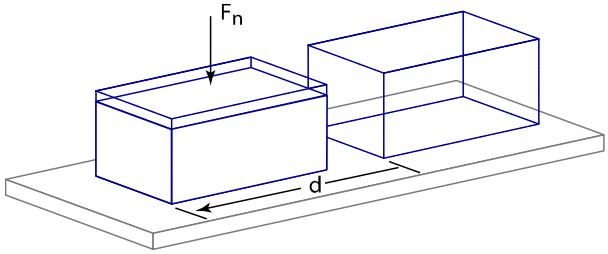

(a) illustrates a wear rate equation

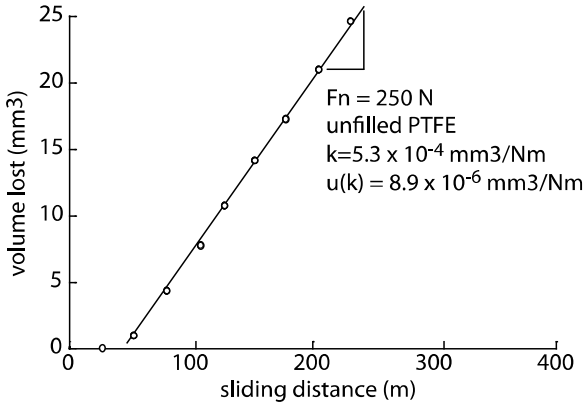

(b) shows data from an unfilled polymer system under steady load

Figure 1. *Wear is the gradual removal of material, which progresses linearly for many material combinations. This common form of wear is often termed mild wear.*

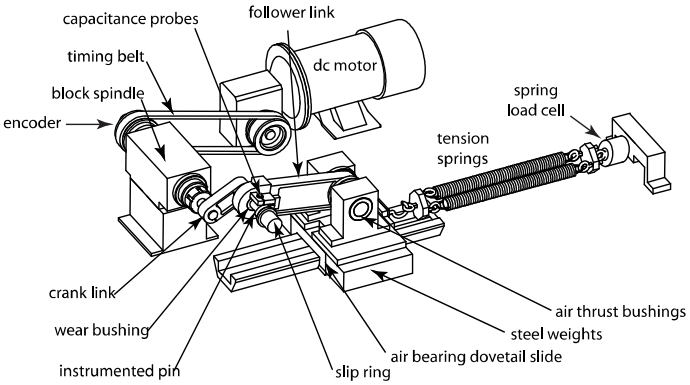

Figure 2. *The layout of slider-crank mechanism used for experiment*

the linear slide, are used.

The revolute joint under study consists of a 19.0mm diameter steel pin and a polymer bushing. The pin is clamped in the crank link at one end and is free to rotate, subject to sliding friction. The bushing is clamped in the follower link. The pin is made of hardened steel and is assumed to be hard enough so that no appreciable wear occurs on its surface. The bushing, on the other hand, is made of poly-tetra-fluoro-ethylene (PTFE) which is soft and is subject to considerable wear. To enable the wear debris to escape the contact area and prevent it from affecting the progression of wear, grooves are machined into the bushing, as shown in Figure 3.

The contact and friction loads experienced by the joint under study can be manipulated in two ways. First, up to 9.6 kg of mass (m_{add}) in the form of steel weights can be bolted to the dovetail slide stage. The corresponding inertial force is dependent on the stage acceleration, which is a function of the stage location and the crank velocity. Additionally, single or dual coil tension springs can be attached in parallel between the stage and the table. With the assumption that the springs have no significant strain rate dependency, the spring force is nominally a function of stage position. Springs used in this study have a nominal spring constant of k_s = 220 N/m. The added mass and springs will attribute to the joint force, which can accelerate the wear progress. In practice, mechanisms are usually operated under added masses and additional constraint

Table 1 *Pertinent slider-crank mechanism parameters. Mass moments of inertia are about the center of mass of each body.*

Property	Value
Crank mass	0.404 kg
Crank moment of inertia	2.0×10^{-4} kg-m^2
Crank length	76.2 mm
Follower mass	0.812 kg
Follower moment of inertia	5.5×10^{-3} kg-m^2
Follower length	203.2 mm
Stage mass	8.5 kg
Pin diameter	19.00 mm

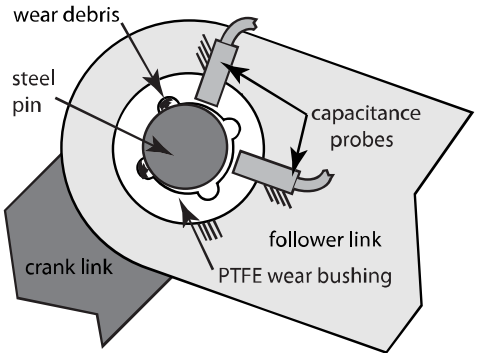

Figure 3. *Capacitance probes measure the location of the pin from fixed locations on the follower link.*

forces. The wear pattern or process depends on three factors: (1) wear coefficient and (2) joint force, and (3) relative motion in the interface. Different joints may have different joint forces and relative motions and they need to be measured. However, the wear coefficient is close to the material property and it is 'almost' independent of the process (wear coefficient is not intrinsic material property). Therefore, the identified wear coefficient for accelerated condition will be close enough to the other conditions.

Forces transmitted through the joint of interest are measured via a load cell built into a steel pin (Figure 4). Two full-bridge arrays of strain gages mounted to a necked-down portion of the pin monitor transverse loads while cancelling out bending stresses. The necked portion of the pin, along with a hollow cross section, also serves to localize the strain to the region where the gages are attached. A slip ring mounted to the free end of the pin allows power and signals to be transmitted to and from the strain gages. The load cell is deadweight calibrated and has a full scale capacity of 400N and a resolution of 2N.

Simultaneously, two orthogonally mounted capacitance probes monitor the position of the pin relative to bushing (Figure 3). These probes are clamped to the follower arm and are electrically insulated by polymer bushings. These probes have a range of 1,250μm and a resolution of 40nm. Additionally, the pin, as the target, is electrically grounded.

Additionally, the angular position of the crank is measured

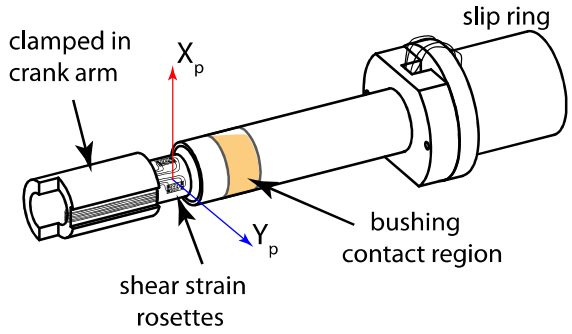

Figure 4. *Instrumented steel pin load cell for measuring joint force.*

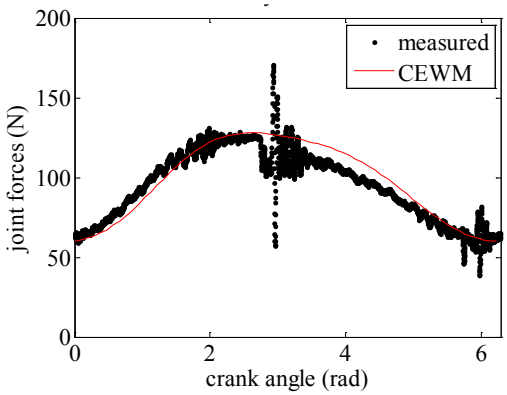

(a) Cycle 1

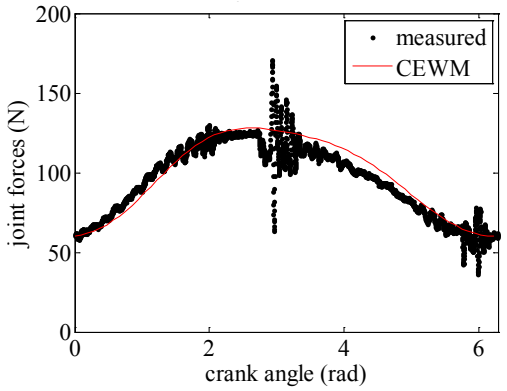

(b) Cycle 20,500

Figure 5. *Joint force predictions and measured data.*

by a hollow shaft incremental encoder attached to the spindle shaft.

Figure 5 shows the joint force as a function of crank angle at Cycle 1 and Cycle 20,500. High frequency oscillation has been observed when the slider changes its velocity direction. However, there is no significant variation of joint forces between different cycles. Thus, the profile of joint forces is fixed throughout entire cycles.

It is well known that uncertainty in applied loading is the most significant factor in prognosis; i.e., without knowing future loadings, the uncertainty in prediction can be so wide that the prediction may not have a significant meaning. This issue can be addressed in two aspects. Firstly, although the loading condition is variable, if there is enough proof that the future loadings will be similar to the past loadings, then the collected data for past joint forces can be used to predict the future loadings. In this case, the future loadings can be represented using statistical method. Of course, the uncertainty in predicted life will be increased due to the added uncertainty. Secondly, the focus of this paper is on characterization of wear parameters, which only depends on the recorded past loading history. Thus, the proposed idea will work for the variable load history, too. In this case, the computation will be more expensive than the current example.

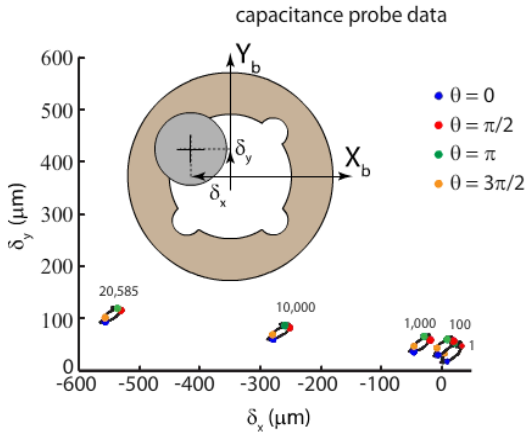

(a) profile of pin center locations

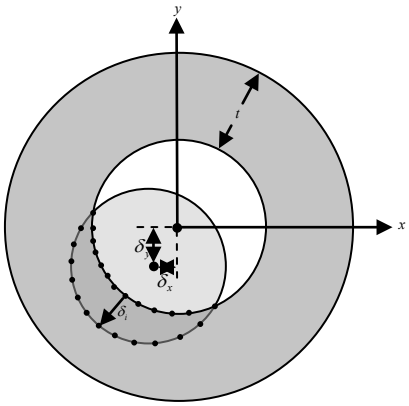

(b) wear volume calculated from the overlapped area

Figure 6. *In-situ measurements of pin displacement.*

Figure 6 shows measured displacements of pin center using the capacitance probe. The wear volume is computed based on the value of δ_x and δ_y. Due to the pre-tensioned springs, the contact points are located only one side of the bushing. However, the location of pin center varies according to crank angle. This can be explained by rounded surface of the pin and different amount of elastic deformation due to variation in spring forces at different angles. The measured forces, computed wear volume from the measured displacement, sliding distance and wear coefficient are shown at 6 sets of number of cycles for crank angles 0 and π radians in Tables 2 and 3, respectively. Although the wear coefficient converges to a value at high cycles, two results converge to different wear coefficient. This is because the joint force is not constant and the measured wear volume includes errors. In the following section, a statistical approach will be introduced to estimate the wear coefficient more reasonably. The idea is to estimate wear coefficient incorporating uncertainty based on the first 5 set of measured data, and predict the wear volume at the future cycle using the information, which is the 6th cycle in Tables 2 and 3. Since the actual data at this cycle are also measured, we can evaluate the reliability or accuracy of the method by comparing the two results.

Table 2 *Wear coefficient calculation using pin locations at 0 radian.*

0 radian				
Cycles	Force	Volume	Slip distance	k x 10^4
1	64.41	1.59	0.06	4134.80
100	62.80	2.57	5.99	68.25
1000	63.17	8.10	59.85	21.44
5000	64.77	24.48	299.24	12.63
10000	62.65	46.21	598.47	12.32
20585	59.96	93.90	1232.00	12.71

Table 3 *Wear coefficient calculation using pin locations at π radian.*

π radian				
Cycles	Force	Volume	Slip distance	k x 10^4
1	103.87	7.29	0.06	11731.00
100	106.90	7.64	5.99	119.43
1000	114.04	9.55	59.85	13.99
5000	138.77	23.87	299.24	5.75
10000	143.50	44.41	598.47	5.17
20585	147.85	91.56	1232.00	5.03

4 BAYESIAN INFERENCE TECHNIQUE FOR PREDICTION OF PROGRESSIVE JOINT WEAR

4.1 Bayes' Theorem

In this study, the Bayesian technique is employed to identify the wear coefficient k, which is the degradation model parameter, by using in-situ measurements data. The method is based on the Bayes' rule as is given by Gelman et al. [8]

$$p(\boldsymbol{\theta}\,|\,\mathbf{y}) \propto L(\mathbf{y}\,|\,\boldsymbol{\theta})\,p(\boldsymbol{\theta}), \tag{4}$$

where $L(\mathbf{y}\,|\,\boldsymbol{\theta})$ is the likelihood of observed data $\mathbf{y}$ which is the wear volume in this case, conditional on the given model parameters $\boldsymbol{\theta}$, $p(\boldsymbol{\theta})$ is the prior distribution of $\boldsymbol{\theta}$, and $p(\boldsymbol{\theta}\,|\,\mathbf{y})$ is the posterior distribution of $\boldsymbol{\theta}$ conditional on $\mathbf{y}$. As more data are provided, the posterior distribution is again used as a prior at the next step, and the values are updated to more confident information. This is called Bayesian updating. The procedure to obtain posterior distribution $p(\boldsymbol{\theta}\,|\,\mathbf{y})$ consists of proper definition of probability distribution for the likelihood and prior respectively, which is outlined as follows.

Since no information in variability of experimental data is available, two types of likelihood are considered: normal and lognormal distributions. In the likelihood calculation, the actual wear volume at a cycle is computed by averaging the values at 0 and π radians (see Tables 2 and 3). Denoting the set of wear volume data obtained at these cycles as $\mathbf{V}$, the likelihoods of the data for given wear coefficient and standard deviation can be defined as

$$L(\mathbf{V}\,|\,k,\sigma) \sim N(\mu,\sigma) \tag{5}$$

$$L(\mathbf{V}\,|\,k,\sigma) \sim LN(\lambda,\zeta) \tag{6}$$

where μ and σ are the mean and standard deviation of the wear volume, and λ and ζ are two parameters of the lognormal distribution. Recalling Eq. (3), the mean wear volume is expressed as the integral of contact force and slip, multiplied by k. In practice, this integral is computed discretely by dividing the cycle into n equal intervals:

$$\mu = kC\left(\sum_{i=1}^{n} F_{n_i}\,\Delta s_i\right) \tag{7}$$

where F_{n_i} and Δs_i are the contact force and incremental slip at i th segment, respectively, and C is the number of cycles. Being the force profile fixed over the entire cycles, the sum in Eq. (7) is obtained as a constant with the value 5.966 [N-m]. In Eq. (6), λ and ζ are given as

$$\lambda = \log\mu + \frac{1}{2}\zeta^2 \quad \text{and} \quad \zeta = \sqrt{\log\left(1+\frac{\sigma^2}{\mu^2}\right)} \tag{8}$$

Note that in Eq. (7), the mean is only the function of k since all other terms are given or fixed. After all, the parameters k and σ are the unknowns to be estimated conditional on the observed data $\mathbf{V}$.

For the prior distribution of k, specific information from the previous literature [9] is employed, which is

$$p(k):\ N(5.05, 0.74)\times 10^{-4} \tag{9}$$

The distribution was obtained from the experiments to determine k for the bushing with the same material as the current study. Non-informative prior assuming no prior knowledge is also considered to study effect of prior information. On the other hand, the prior distribution of σ is considered as non-informative prior.

Consequently, the posterior PDF of wear coefficient k is obtained by multiplying Eq. (5) or Eq. (6) and the prior distribution $p(k)$ in Eq. (9).

4.2 MCMC Simulation

Once the expression for posterior PDF is available, one can proceed to sample from the PDF. A primitive way is to compute the values at a grid of points after identifying the effective range, and to sample by the inverse CDF method. This method, however, has several drawbacks such as the difficulty in finding correct location and scale of the grid points, spacing of the grid, and so on. MCMC simulation is an effective solution in this case [10]. The Metropolis-Hastings (M-H) algorithm is typical method of MCMC, which is given in Table 4.

Table 4 *MCMC simulation process*

1. Initialize $\left[k^{(0)},\sigma^{(0)}\right]$.

2. For $i=0$ to $N-1$

– Sample $u \sim U_{[0,1]}$.

– Sample $\left[k^{*},\sigma^{*}\right] \sim q\left(k^{*},\sigma^{*} \mid k^{(i)},\sigma^{(i)}\right)$.

– if $u < A\left(\left[k^{(i)},\sigma^{(i)}\right],\left[k^{*},\sigma^{*}\right]\right)$

$$\left(A = \min\left\{1, \frac{p\left(k^{*},\sigma^{*}\right) q\left(k^{(i)},\sigma^{(i)} \mid k^{*},\sigma^{*}\right)}{p\left(k^{(i)},\sigma^{(i)}\right) q\left(k^{*},\sigma^{*} \mid k^{(i)},\sigma^{(i)}\right)}\right\} \right)$$

$$\left[k^{(i+1)},\sigma^{(i+1)}\right] = \left[k^{*},\sigma^{*}\right]$$

else

$$\left[k^{(i+1)},\sigma^{(i+1)}\right] = \left[k^{(i)},\sigma^{(i)}\right]$$

In Table 4, $\left[k^{(0)},\sigma^{(0)}\right]$ are the initial values of unknown parameters to be estimated, N is the number of iterations or samples, U is the uniform distribution, $p(x)$ is the posterior PDF (target PDF), and $q(x)$ is an arbitrary chosen proposal distribution. A uniform distribution is used in this study for the sake of simplicity. Then, $q\left(k^{(i)},\sigma^{(i)} \mid k^{*},\sigma^{*}\right)$ and $q\left(k^{*},\sigma^{*} \mid k^{(i)},\sigma^{(i)}\right)$ become constant, and $q(k,\sigma)$ can be ignored. As an example of MCMC, Figure 7 and Table 5 show the sampling result of k,σ of which the posterior PDF given as

$$p(k,\sigma) \propto \left(\frac{1}{\sqrt{2\pi}\sigma}\right)^{5} \exp\left[-\frac{1}{2}\sum_{i=1}^{5}\frac{\left(V_i - kF_n s\right)^2}{\sigma^2}\right] \qquad (10)$$

With only 10,000 iterations, the sampling result follows the distribution quite well.

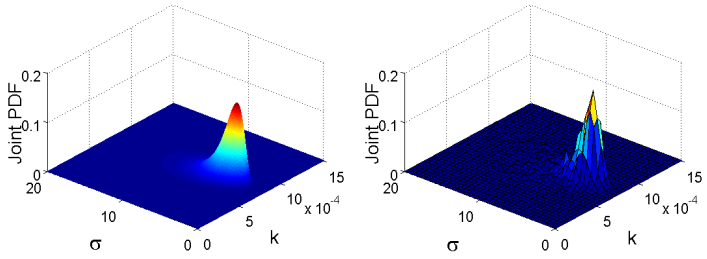

(a) exact solution (b) using MCMC

Figure 7. *Joint posterior PDF*

Table 5 *Statistical moments*

	Eμ	Eσ	E$\mu\mu$	E$\sigma\sigma$	E$\mu\sigma$
Exact Sol.	7.7597	5.6321	0.8478	6.3045	0
MCMC	7.8212	5.6055	0.8613	6.7054	0
Error (%)	0.79	0.47	1.60	6.36	0

5 IDENTIFICATION OF WEAR COEFFICIENT AND PREDICTION OF WEAR VOLUME

5.1 Posterior Distribution of Wear Coefficient

The posterior distributions of k and σ are obtained using the MCMC technique with the first 5 sets of data in Tables 2 and 3. In the MCMC process, the number of iterations is fixed at 10,000. During the iteration, determining the convergence condition is a difficult task because there is no clearcut criterion, but certain amount of experience is required. It involves discarding the values at the initial stage of the iteration, and monitoring the traces and histogram plots at the later part of the iteration from which the subjective judgment is made as to the convergence to a stationary chain. The resulting

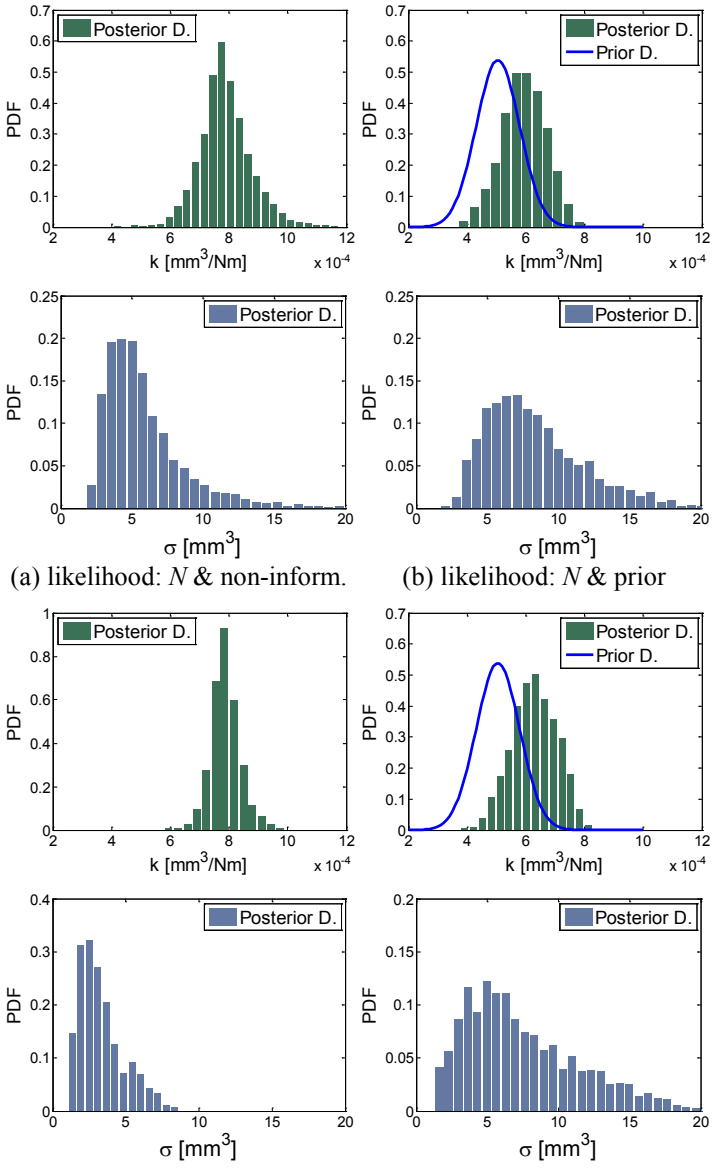

(a) likelihood: N & non-inform. (b) likelihood: N & prior

(c) likelihood: L & non-inform. (d) likelihood: L & prior

Figure 8. *Posterior distribution when using data=5.*

Table 6 *Mean and standard deviation of k* (10^{-4} mm^3/Nm).

		Num.of data set	3	4	5	6
normal	non-inform.	mean	17.49	8.28	7.89	7.57
		std.	10.02	2.32	0.90	0.40
	prior	mean	5.11	5.42	5.93	6.89
		std.	0.73	0.73	0.76	0.57
lognormal	non-inform.	mean	20.81	8.89	7.88	7.64
		std.	5.82	1.17	0.51	0.25
	prior	mean	5.46	5.67	6.29	7.41
		std.	0.72	0.75	0.77	0.25

PDF's are given in Figure 8. Both normal and lognormal distributions are considered for the likelihood, and both non-informative and normal distribution are considered for the prior. In the case of non-informative prior, the PDF shape (c) of lognormal likelihood is narrower than the shape (a) of normal likelihood. As shown in the 5th set of Table 6, the standard deviation from the lognormal likelihood (0.51×10^{-4} mm^3/Nm) is 43% less than that of normal likelihood (0.9×10^{-4} mm^3/Nm) whereas the mean values are nearly equal, i.e., 7.89 and 7.88. The results show that the lognormal likelihood exhibits superior precision to the normal likelihood. The reason that the lognormal likelihood is better than the normal may be attributed to the non-negativity of the lognormal distribution, which is the case of the wear coefficient. Comparing the results by the two priors, i.e., (a) vs (b) and (c) vs (d), use of the prior leads to the estimation of smaller mean for k. It is noted that the actual k values at the last cycle are found to vary between 5.03×10^{-4} and 12.71×10^{-4} (see Tables 2 and 3), of which the average is 8.5×10^{-4}. Despite employing prior, the results are worse than the non-informative results. This may happen because the prior distribution is not accurate. As mentioned before, the tribometer wear tests are performed under the uniform pressure condition, while the contact pressure in the bushing is not constant.

In order to investigate the effect of prior in more detail, the posterior distributions of k are obtained after updating at each stage of data set. Values of the mean and standard deviation are given in Table 6, and 5%, 95% percentile and MLE values are plotted in Figure 9, respectively. In Figure 9, the green line denotes the mean value of the distribution after the last update, i.e., using the 6th data set. This is used as a target value for correct prediction of the earlier stage.

In Figure 9(a) and 9(b), the confidence intervals with prior are located much lower than the ones without prior, and do not include the target value. Remark from these observations is that although the use of prior knowledge is usually recommended to accommodate more confidence and faster convergence, it should be used in caution. In this study, the wear coefficient is not intrinsic material property but can vary with operating condition. This turned out to be the cause of incorrect prediction, and should be avoided. It should be noted however that this is not always the case. If only a limited data are available unlike the present case, user may have to depend more on the prior knowledge than the likelihood of the data.

5.2 Posterior Prediction of Wear Volume

Once the posterior distribution of k and σ are obtained, the information can be used to predict the wear volume at the future stage. For that purpose, the wear volume at 6th data set (20,585 cycles) is predicted using the posterior distribution of wear coefficient at each cycle. The predictive distribution of wear volume are computed using the posterior distribution of k and σ at each stage, and 5%, 95% and MLE values are plotted in Figure 10. In the figure, the actual value of wear volume measured at the 6th data set is used as a target value which is 92.73 mm^3. As was noted before, the use of prior does not predict the wear volume well. Besides, even the upper confidence limit is below the target value, which can cause unexpected failure if the value is carelessly used in the design decision.

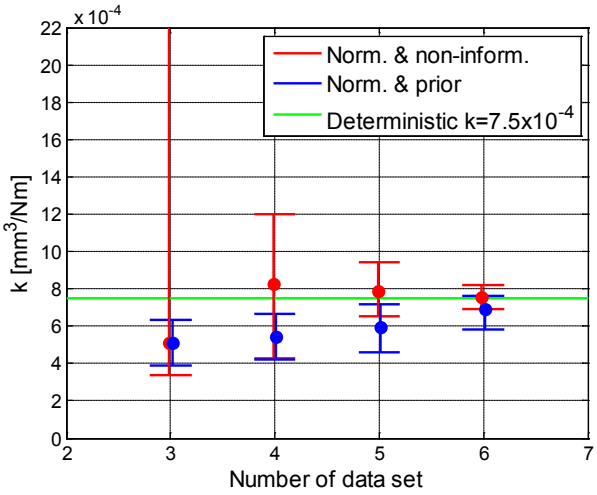

(a) likelihood: Normal distribution

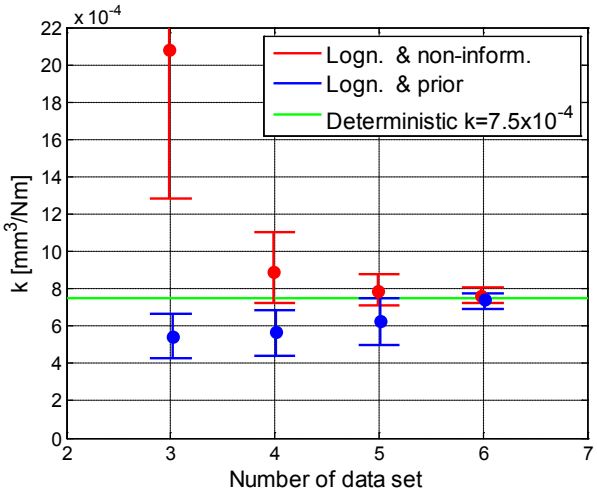

(b) likelihood: Lognormal distribution

Figure 9. *P values in terms of number of data set.*

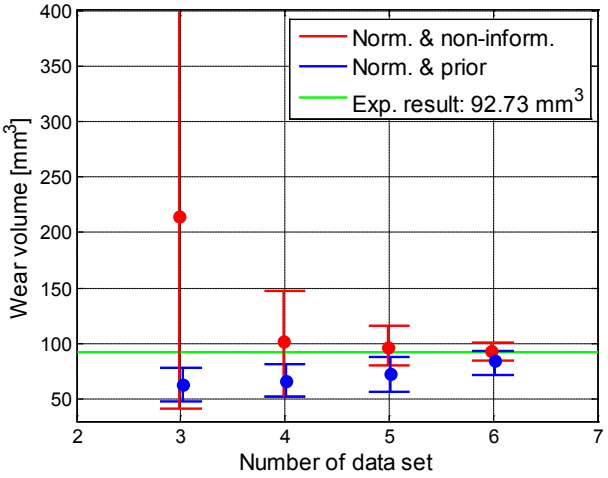

(a) likelihood: Normal distribution

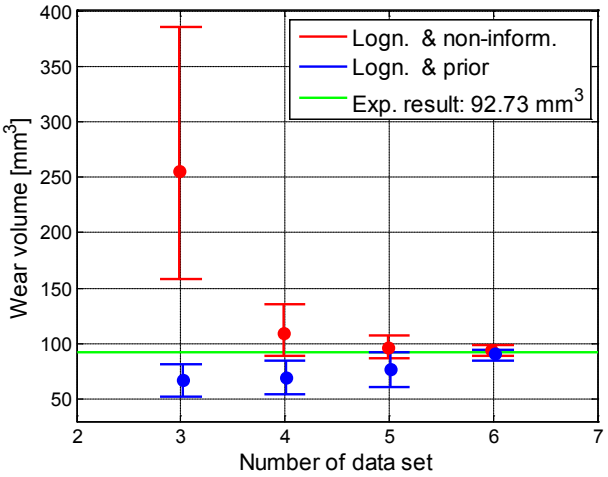

(b) likelihood: Lognormal distribution

Figure 10. *Wear volume prediction in terms of number of data set.*

Comparing the results of normal and lognormal likelihood, the length of interval is quite larger at the 3rd stage of data in the case of normal likelihood. But the lengths of the intervals are quickly reduced and get closer each other afterwards as the number of cycles increases. Overall, the lengths of interval of the lognormal case are smaller than the other.

In Figure 11, predictive distribution of the wear volume at the 6th stage using the posterior distribution of 5th stage are given, in which the red line denotes the actual measured value. The result of non-informative prior are better than the case of prior.

In Figure 12, the confidence interval (CI) and predictive intervals (PI) of the wear volumes at all the stages are given using the posterior distribution of 5th stage along with the actual measured data denoted by green dots. In the case of the lognormal likelihood, the results at the 1st and 2nd stages, which are 1 cycle and 100 cycles respectively, exhibit very small intervals and do not include the actual points, which are inadequate. The reason is due to the larger uncertainty at the early stage with small data while the lognormal distribution

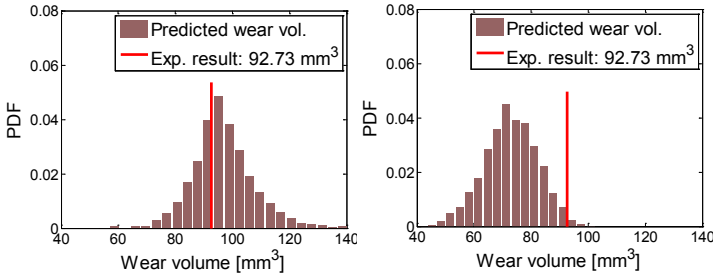

(a) likelihood: *N* & non-inform. (b) likelihood: *N* & prior

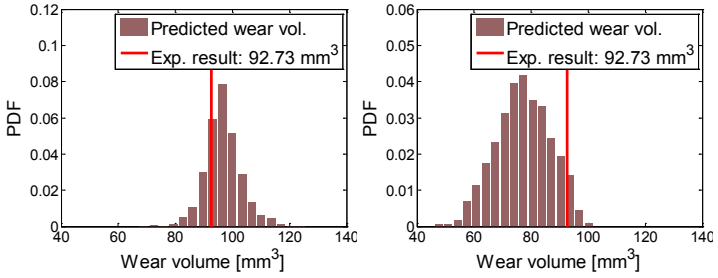

(c) likelihood: *L* & non-inform. (d) likelihood: *L* & prior

Figure 11. *Wear volume prediction.*

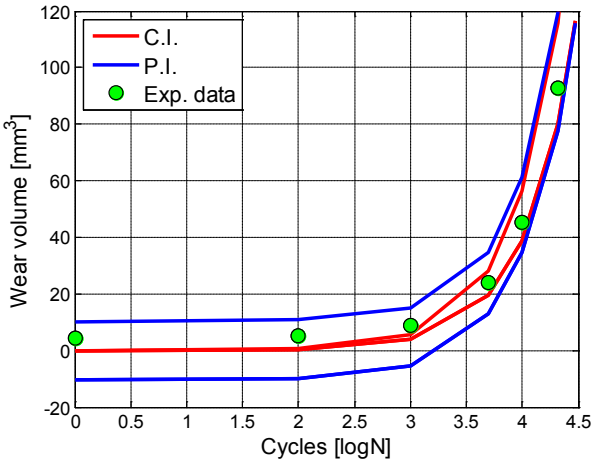

(a) likelihood: Nnormal distribution

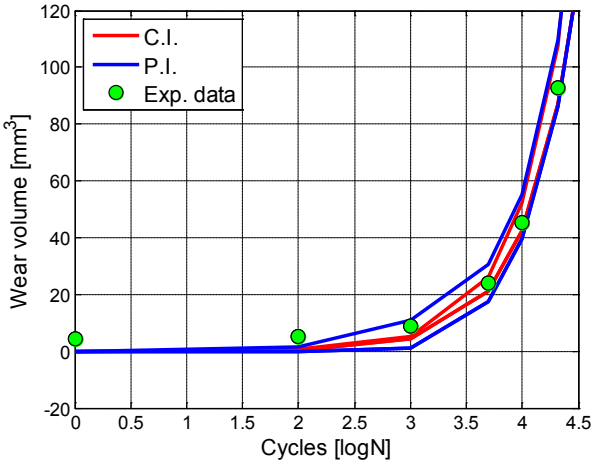

(b) likelihood: Lognormal distribution

Figure 12. *C.I. and P.I. of wear volume.*

Table 7 *C.I. and P.I. of wear volume.*

	Num.of data set		1	2	3	4	5	6
true wear V			**4.44**	**5.105**	**8.825**	**24.175**	**45.31**	**92.73**
C. I.	N	95%	0.01	0.56	5.63	28.13	56.25	115.80
		5%	0.00	0.39	3.89	19.43	38.87	80.01
		inter	0.00	0.17	1.74	8.69	17.39	35.79
	L	95%	0.01	0.52	5.23	26.14	52.27	107.60
		5%	0.00	0.42	4.23	21.16	42.31	87.10
		inter	0.00	0.10	1.00	4.98	9.96	20.50
P. I.	N	95%	10.62	10.47	15.25	34.53	60.72	118.80
		5%	-10.24	-9.51	-5.33	12.72	33.87	77.49
		inter	20.85	19.98	20.58	21.81	26.85	41.31
	L	95%	0.00	1.74	10.59	30.03	55.03	108.84
		5%	0.00	0.00	1.13	17.60	40.00	85.62
		inter	0.00	1.74	9.46	12.43	15.03	23.21

does not allow negative values. Nevertheless, these early stages are not of the interest in terms of prognosis. In Table 7, the numerical values of CI and PI are shown as well. The values are different significantly at the early stage, i.e., at the 1st and 2nd stages, due to the same reason as mentioned above, hence, is insignificant. From 1,000 cycles, which is the 3rd stage, the CI's and PI's of lognormal case is smaller than the normal case, which demonstrates superior precision.

6 CONCLUSIONS AND DISCUSSIONS

In this paper, the Bayesian inference technique is utilized to estimate the probability distribution of wear coefficient using in-situ measurements. The first five data up to 10,000 cycles are used to reduce uncertainty in wear coefficient, and the last data at 20,585 cycles are used for validation purpose. The numerical results show that the posterior distribution with non-informative is more accurate than that with the prior distribution from the literature. This happens because the converged posterior distribution is quite different from the prior distribution. In order to predict the wear coefficient of a mechanical component, it has been suggested that the wear volume, slip distance and applied load must be measured simultaneously.

ACKNOWLEDGMENTS

This work was supported by the National Research Foundation of Korea (NRF) grant funded by the Korea government (MEST) (No. 2009-0081438, No. 2008-02-010), Deere and Company, and National Science Foundation (CMMI-0600375).

REFERENCES

1. N. H. Kim , D. Won , D. Buris, B. Holtkamp, G. R. Gessel, P. Swanson, W. G. Sawyer, Finite Element Analysis and Validation of Metal/Metal Wear in Oscillatory Contacts, Wear, Vol. 258, No. 11-12, pp. 1787–1793, 2005.
2. S. Mukras, N. H. Kim, and N. A. Mauntler, T. Schmitz, and W. G. Sawyer, Analysis of planar multibody systems with revolute joint wear, Wear, Vol. 268, No. 5-6, pp. 643–652, 2010.
3. N. Mauntler, N. H. Kim, W. G. Sawyer, T. L. Schmitz, An instrumented crank-slider mechanism for validation of a combined finite element and wear model, Proceedings of 22nd Annual Meeting of American Society of Precision Engineering, October 14 - 19, 2007, Dallas, Texas.
4. J.F. Archard, Contact and rubbing of flat surfaces. Journal of Applied Physics 24 (1953) 981-988.
5. S.C. Lim, and M.F. Ashby, Wear-mechanism maps. Acta Metall 35 (1987) 1-24.
6. A. Cantizano, A. Carnicero, and G. Zavarise, Numerical simulation of wear-mechanism maps. Computational materials science 25 (2002) 54-60.
7. R. Holm, Electric Contacts. 1946, Uppsala: Almqvist & Wiksells Boktryckeri.
8. Gelman, A., J. B. Carlim, H. S. Stern, and D. B. Rubin. Bayesian Data Analysis (second ed.). New York, Chapman & Hall/CRC, 2004
9. T.L. Schmitz, J.E. Action, D. L. Burris, J.C. Ziegert, W.G. Sawyer, Wear-rate uncertainty analysis, Wear 126 (2004) 802–808.
10. Andrieu, C., N. de Freitas, A. Doucet, and M. Jordan. An introduction to MCMC for Machine Learning. Machine Learning, 50:5-43, 2003